



OPEN

Biologically inspired band-edge laser action from semiconductor with dipole-forbidden band-gap transition

SUBJECT AREAS:

BIOLOGICAL
FLUORESCENCELASERS, LEDS AND LIGHT
SOURCESCih-Su Wang¹, Chi-Shung Liao¹, Tzu-Ming Sun¹, Yu-Chia Chen¹, Tai-Yuan Lin² & Yang-Fang Chen¹Received
25 November 2014Accepted
12 February 2015Published
11 March 2015Correspondence and
requests for materials
should be addressed to
Y.-F.C. (yfchen@phys.
ntu.edu.tw)¹Department of Physics, National Taiwan University, Taipei 106, Taiwan, ²Institute of Optoelectronic Sciences, National Taiwan Ocean University, Keelung 202, Taiwan.

A new approach is proposed to light up band-edge stimulated emission arising from a semiconductor with dipole-forbidden band-gap transition. To illustrate our working principle, here we demonstrate the feasibility on the composite of SnO₂ nanowires (NWs) and chicken albumen. SnO₂ NWs, which merely emit visible defect emission, are observed to generate a strong ultraviolet fluorescence centered at 387 nm assisted by chicken albumen at room temperature. In addition, a stunning laser action is further discovered in the albumen/SnO₂ NWs composite system. The underlying mechanism is interpreted in terms of the fluorescence resonance energy transfer (FRET) from the chicken albumen protein to SnO₂ NWs. More importantly, the giant oscillator strength of shallow defect states, which is served orders of magnitude larger than that of the free exciton, plays a decisive role. Our approach therefore shows that bio-materials exhibit a great potential in applications for novel light emitters, which may open up a new avenue for the development of bio-inspired optoelectronic devices.

In recent years, there's a growing interest to develop laser-based photonic technologies, which have made a tremendous impact on modern science and medical applications, such as sensing and diagnosis¹. Semiconductor nanowires (NWs) possess several unique electronic and optical properties due to the cylindrical geometry and two-dimensional confinement of electrons and holes, which make them particularly attractive as potential building blocks for nanoscale optoelectronic devices, including light emitting diodes and lasers². As an active photonic device, lasers are composed of a pumped gain medium placed within an optical resonator. Based on these two elements, semiconductor nanowires not only serve as a gain medium but a cavity as well for laser action. Simultaneously, the large refractive index of semiconductors and wire-like geometry enable strongly scattering process existed in the NWs system, and the constructive interference effect consequently results in optical coherent feedback for the outcome lasing modes. Room-temperature lasing has been readily achieved in ZnO, GaN, GaAs and CdSe nanowires due to their large exciton binding energy³⁻⁷. Fruitful derivatives are also promising in wide fields such as biosensors, transistors, gas sensors and solar cells⁸⁻¹¹. Among the functional wide-bandgap semiconductors, only limited progress has been made in the field of ultraviolet tin dioxide (SnO₂) nanowire lasers. Although SnO₂ has a wide direct bandgap (3.6 eV) and large exciton-binding energy (130 meV), it is so far commonly believed that SnO₂ is not a suitable ultraviolet (UV) luminescent material due to the dipole-forbidden nature of its bandgap quantum states¹². Generally, only a broad visible oxygen defect photoluminescence (PL) is observed in most of the reports, since the even-parity symmetry of the conduction band and valence band states in SnO₂ prohibits the bandgap radiative transition¹². Until now, only a little attention has been paid to the research for bringing up the related mechanism of SnO₂ photoemission in ultraviolet range, the underlying origins still remain as an issue of debates^{13,14}. More theoretical insights are still in need. However, in order to achieve a better UV performance of SnO₂ NWs and overcome the difficulties for future coming applications, an improvement for the external conversion efficiency is essential and now paramount.

Chicken egg white (albumen), as a kind of ubiquitous nutritious food in our daily life can serve as a new excellent UV-emitting (~340 nm) protein. Compared with traditional laser dyes (e.g. rhodamine 6G (R6G)), the advantages of chicken albumen consist of the biodegradable, bioresorbable and biocompatible characteristics. More attractive, it is cost-effective and environmentally friendly. Very recently, related research has been paid to the field of modern organic optoelectronics, such as light emitters and field effect transistors (FET)^{15,16}. As a new generation of efficient emitting biomolecule, chicken albumen is expected to be potential for future green technologies.



In this paper, we demonstrate, for the first time a facile and practical strategy to fabricate a newly designed organic-inorganic hybrids composite based on chicken albumen/SnO₂ NWs. Quite surprisingly, it is observed that the originally undetectable UV fluorescence (387 nm) in pristine SnO₂ NWs can be drastically enhanced in the albumen/SnO₂ NWs composite. More excitingly, via effective optical excitation, the coherent laser action can be further sustained and derived. Our strategy to overcome the UV-light-emitting drawback of SnO₂ NWs is based on the fluorescence resonance energy transfer (FRET). FRET is a physical phenomenon where excitation energy from an excited donor (chicken albumen) is non-radiatively transferred to a proximal ground-state acceptor (SnO₂ NWs), and the energy transfer process in a FRET system requires good overlap between optical transition bands of donor and acceptor as well¹⁷. As reported, FRET has been shown to be sufficiently applicable to a variety of biological systems¹⁸. Our proposed unprecedented FRET-assisted UV-emitting laser device based on albumen/SnO₂ NWs composite is not only simple but also paves an excellent alternative way of utilizing chicken albumen protein, which may enable to trigger the further development of bio-inspired optoelectronic devices.

Results

Morphology and optical characterization of SnO₂ NWs and chicken albumen. Figure 1(a) shows the top view SEM image of the as-synthesized SnO₂ NWs. It is observed that the nanowires are randomly assembled and closely packed. An inset of Fig. 1(a) reveals a closer view on SnO₂ NWs. The average length is of about 10 μm, while the diameter is ranging between 70 nm and 150 nm. The XRD pattern of the as-prepared SnO₂ NWs is shown in Fig. 1(c). It can be seen that all peaks are perfectly indexed to the tetragonal rutile SnO₂. As additional evidence, a Raman scattering spectrum is shown in Fig. 1(d), in which the three peaks at 475, 630, 768 cm⁻¹ correspond to the E_g, A_{1g}, and B_{2g} vibration modes, respectively. All these informations further confirm the existence of the as-grown SnO NWs. For the optical properties, a PL spectrum is first characterized as shown in Fig. 1(b). We can clearly see that only a broad orange emission peak located at 625 nm (2.0 eV) is observed, and no ultraviolet fluorescence can be detected. The detected visible light arising from SnO₂ is generally believed to stem from the deep-trapped state, which is related to the oxygen vacancies (O_v) or tin interstitials (Sn_i)¹⁴. Figure 2 presents the PL spectra for both of the pristine SnO₂ NWs and chicken albumen. The UV emission arising

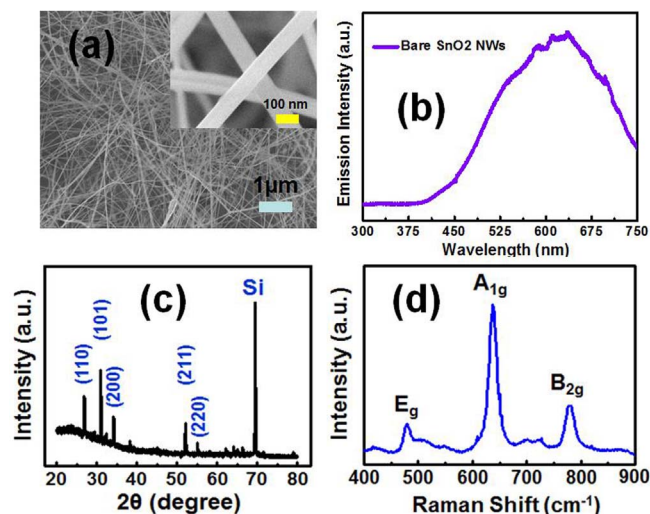


Figure 1 | (a) Scanning electron microscope (SEM) image of the as-grown pristine SnO₂ nanowires (NWs). The inset shows a closer SEM image. (b) Photoluminescence of SnO₂ NWs. (c) X-ray diffraction pattern of SnO₂ NWs. (d) Raman scattering spectrum of SnO₂ NWs.

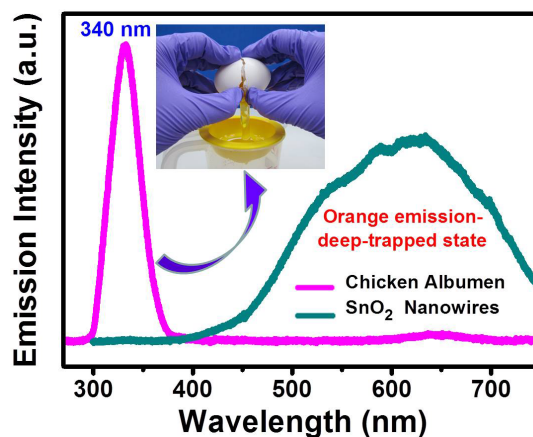


Figure 2 | Photoluminescence spectra of chicken albumen (340 nm) and bare SnO₂ NWs (625 nm). The inset illustrates the separation of egg white (albumen) and egg yolk. (The photograph of the inset was taken by the first author Cih-Su Wang.).

from albumen is centered at around 340 nm, and the FWHM is much narrower compared with that of the bare SnO₂ NWs. It is found that the optical property for albumen is quite stable even under the UV laser pumping. At the beginning, the albumen was spin-coated on a cleaned glass substrate for the PL measurement. The first sample was then stored and preserved in a Petri dish at room temperature. More than our expectation, the PL can still be detected and shown to be stable even after 6 months. Based on these characteristics, albumen from chicken egg reveals one of its advantages as an excellent UV-emitting biomolecule. The inset of Fig. 2 illustrates the separation of egg white (albumen) and egg yolk. In addition to the fluorescence properties, the transmittance spectra of albumen with different spin-coating speed were also shown in Fig. 3. The film thicknesses are about 800 nm (1000 rpm) and 400 nm (5000 rpm), respectively. Both the albumen samples with different thickness show similar transmission properties which indicate good transparency from ultraviolet to visible range. The inset of Fig. 3 shows the topological AFM of the albumen surface, and the root mean square (RMS) roughness is 0.34 nm.

Photoluminescence and laser action of albumen/SnO₂ NWs composite. Figure 4 shows the PL spectrum of the organic-inorganic hybrid structure of albumen/SnO₂ NWs composite. At the beginning, no ultraviolet fluorescence can be ever detected

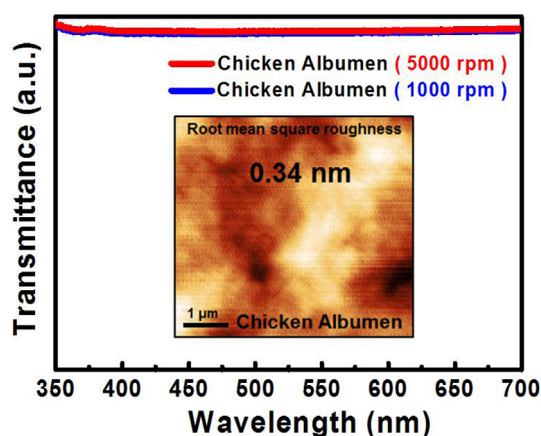


Figure 3 | Transmittance spectra of pristine albumen under different spin-coating speed. The inset shows the atomic force microscope image of albumen surface.

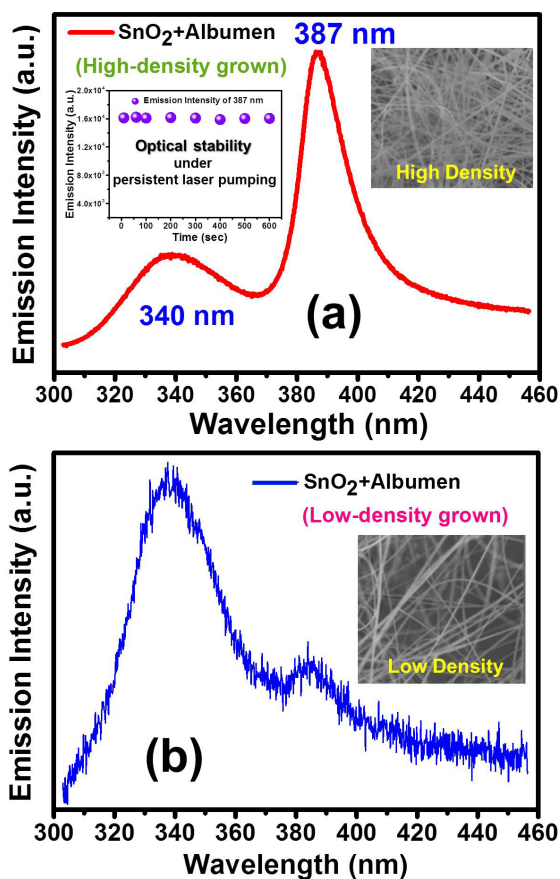


Figure 4 | Photoluminescence (PL) spectra of albumen-coated SnO₂ nanowires (NWs) both for (a) high-density and (b) low density-grown SnO₂ NWs. The left inset of Fig. 4(a) shows the PL intensity of 387 nm as a function of time. The rest insets show the scanning electron microscope images of SnO₂ NWs without albumen coating.

from the as-synthesized bare SnO₂ NWs. However, to our astonishment, when chicken albumen is spin-coated (5000 rpm) onto the SnO₂ NWs, two UV emission peaks located at the positions of 340 nm and 387 nm emerge. Similar result can both be found in high-density (Fig. 4(a)) and low-density (Fig. 4(b)) grown SnO₂ NWs coated by albumen. The 340 nm emission is indexed to the existing albumen covered on SnO₂ NWs, and is basically the same as prior shown in Fig. 2. Compared with the albumen emission, we are more intriguing to characterize the new emerging 387 nm UV fluorescence. Tin dioxide is a direct bandgap semiconductor, however, limited by its dipole-forbidden nature, the bandgap emission with the photon energy of 3.6 eV (~344 nm) is prohibited at room temperature due to the selection rule¹⁴. In addition to the former described deep-trapped state (~2.0 eV) resulting in the visible light, a shallow-trapped state (3.2 eV) within the bandgap of SnO₂ has also been found¹⁴. Via the comparison of Figs. 4(a) and 4(b), it is apparent that the photoemission of 387 nm strongly depends on the density of SnO₂ NWs, and decreases as the NWs turn to be sparse. Herein, the observed UV fluorescence centered at 387 nm (3.2 eV) is believed due to the shallow state of SnO₂ NWs as shown in the early reports^{4,13,14}. To test the photo-stability of the emission of 387 nm from the albumen/SnO₂ composite, the PL intensity was measured at regular time interval under a persistent laser pumping with fixed energy (left inset of Fig. 4(a)). All the recorded data remained in the same order of magnitude with a considerable stability of more than 600 sec. Therefore, an excellent photo-stability of our sample is further confirmed for practical applications. It is worth noting that

the visible defect emission of SnO₂ NWs remains nearly the same before and after albumen coating. Since the visible emission is mainly due to the oxygen vacancies and independent of the albumen coating, the emission spectra are therefore not shown here. The rest right insets of Fig. 4 show the SEM images of dense and sparse SnO₂ NWs without albumen coating. Concerning that the SnO₂ NWs are randomly assembled, the coating of albumen might be partially uneven. However, supported by the transmittance spectra in Fig. 2, the similar fine transparency of albumen both for 1000 rpm and 5000 rpm indicates that the thickness effect on the intensity of the photoemission (387 nm) can be fairly ignored.

In order to interpret the enhancement of 387 nm UV emission, the fluorescence resonance energy transfer (FRET) is believed to be the most possible underlying mechanism. For the occurrence of FRET, donor should be located in the close proximity of acceptor. Meanwhile, a good overlap is required between the optical transition bands of donor and acceptor. In our study, the donor and acceptor are albumen protein and SnO₂ NWs, respectively. According to the previous reports^{15,19,20}, the absorption spectra of albumen and SnO₂ exhibit a good overlap ranging from 250 nm to 300 nm. It is well documented that the strong optical absorption in albumen is at around 3.65 eV, while that of SnO₂ occurs at 3.6 eV. Therefore, the newly designed albumen/SnO₂ NWs composite is well feasible for the proposed FRET mechanism, in which the energy can be efficiently transferred from albumen protein to SnO₂ NWs. Figure 5 illustrates the band alignment diagram, which provides a clear physical picture to describe the FRET process between chicken albumen and SnO₂ NWs via two dominant steps. First, in Fig. 5(a), due to the good overlap between the absorption bands of albumen and SnO₂, the energy absorbed by the albumen protein can be easily transferred to SnO₂ NWs through the resonant FRET effect. Second, the 340 nm UV transition arising from Tryptophan in albumen also shows an excellent overlap with the bandedge transition of 344 nm in SnO₂ NWs thus supports the origin of FRET as well. However, limited by the direct-forbidden nature, the bandgap emission with the photon energy of 3.6 eV is prohibited. Therefore, the excited carriers will transfer to the nearest shallow-trapped state and result in the UV fluorescence with the wavelength of 387 nm (3.2 eV). Based on the above proposed mechanisms, the PL spectra shown in Fig. 4 can now be well interpreted.

Lasing occurs in a cavity by stimulated emission, which provides optical amplification¹. Herein, the coherent optical transition within the bandedge of gain medium is important. For the occurrence of deep-trapped recombination in SnO₂ NWs, the long decay time makes it not capable to block the fast coherent radiation of bond excitons. On the contrary, the excited carriers are much more efficient to bind and populate into the shallow trapped states, and emit photons with a fast decay rate¹⁴. Hence, the laser action amplified by coherent stimulated emission can be expected in the albumen/SnO₂ NWs system at the wavelength of 387 nm rather than the visible range. To confirm our expectation, the albumen/SnO₂ NWs composite were optically pumped by the Q-switched Nd: YAG laser (266 nm, 3–5 ns pulse, 10 Hz) for the lasing study. Series of fluorescence spectrum under different excitation energy were performed as shown in Figs. 6(a)–(d). At a low pumping power such as 40 μJ, the PL spectrum is broad and featureless (Fig. 6(a)). However, when the pumping energy exceeds a specific threshold of 45 μJ (Fig. 7), a sharp lasing peak at around 387 nm with the line width (FWHM) less than 1.3 nm starts to emerge. The rapid increase of fluorescence intensity indicates that the stimulated emission occurs in the hybrid system. As the pumping energy goes higher, the more output lasing modes appear around the wavelength of 387 nm. It is worth noting that the albumen emission located around 340 nm shows a reduction as the lasing peaks and intensity grow. As additional evidence, the reduction further supports the strong energy transfer from albumen protein to SnO₂ NWs via the proposed resonant FRET effect.

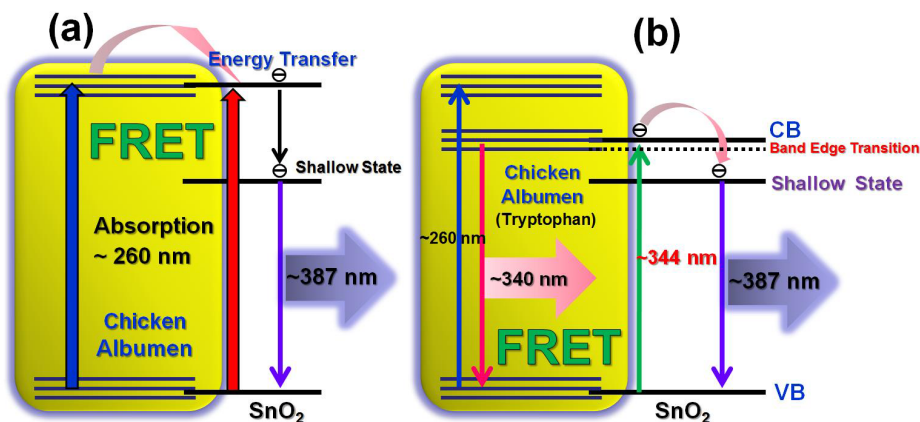


Figure 5 | (a), (b) Illustration for the physical picture of fluorescence resonance energy transfer process existing between albumen protein and SnO₂ nanowires.

Discussion

For the occurrence of laser action in our study, Fabry-Perot (FP) and Whispering Gallery Mode (WGM) types will not be considered as main mechanisms, since the former requires highly oriented vertical nanowire array providing flat facets in both ends as an optical cavity, while the later needs spherical or hexagonal shape cavity as a confinement of light^{21,22}. It is believed that the dominant mechanism can be interpreted by the random lasers (RLs). RL consists of a randomly distributed structures dispersed into an optical gain medium, in which the closed-loop path (optical cavity) is merely provided by multiple scattering process of light²³. Therefore, the randomly assemble tetragonal SnO₂ NWs are well feasible for the occurrence of RL. By using the information of the wavelength difference ($\Delta\lambda$) derived from the two nearest lasing peaks, the scattering mean free path (L) of a light in the composite system can be calculated by $L = \lambda^2/2n\Delta\lambda$ ²⁴, where λ is the resonant wavelength (~ 387 nm), n is the

refractive index (~ 2), L is the resonant cavity length, and the approximate value is about 23.4 μm . Besides, the varied lasing modes and intensity under different pumping further confirm the RL existence in the albumen/SnO₂ NWs composite, since the random cavity made by closed-loop path changes every moment. It should be noted that RL derived from the albumen/SnO₂ NWs composite contains only few peaks compared with the early reports⁴. This may be explained by the reduction of scattering strength since the refractive index of albumen ($n \sim 1.35$) is less than that of the SnO₂ NWs ($n \sim 2.0$)²⁵, as well as by the narrow spectrum due to the shallow trapped state¹⁴. The advantage of mode reduction leads to the possibility of mode controlling and towards mode locking for the future RL applications. The emission peak intensity as a function of pumping energy is shown in Fig. 7, from which the threshold (P_{th}) of about 45 μJ can be derived. The inset of Fig. 7 illustrates the closed-loop path inside nanowires. It is intriguing to further realize why the shallow-trapped

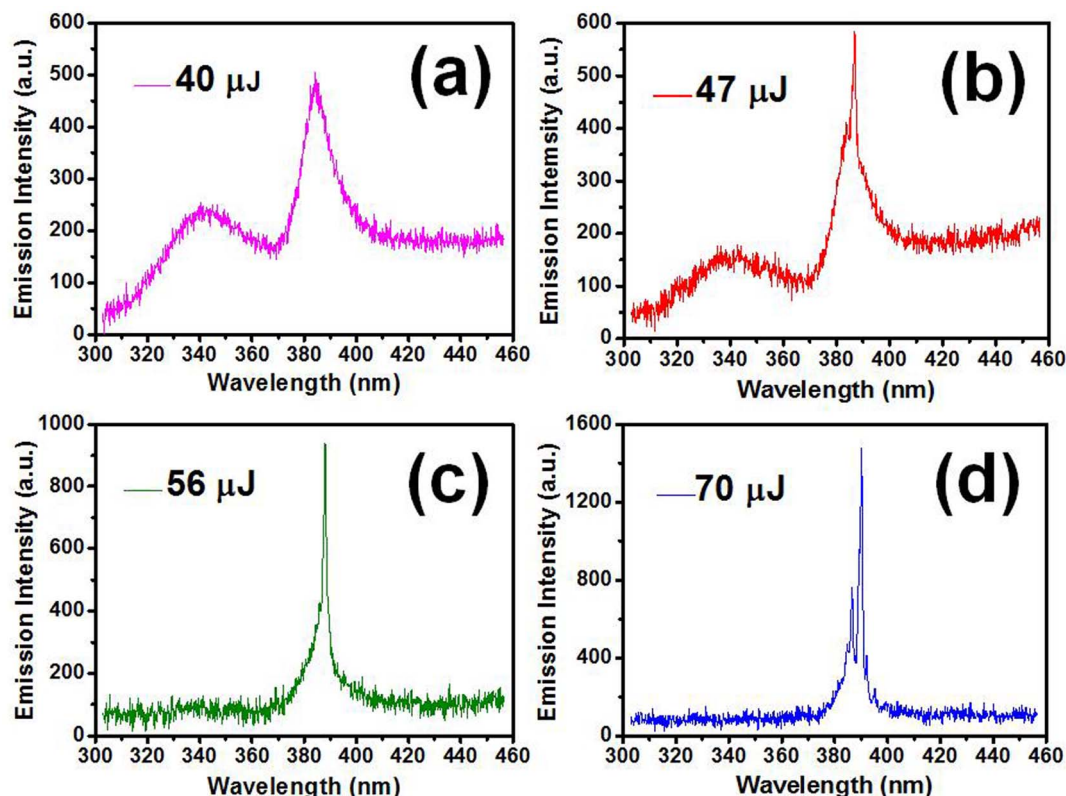


Figure 6 | Laser actions of albumen-coated SnO₂ nanowires under different excitation energy.

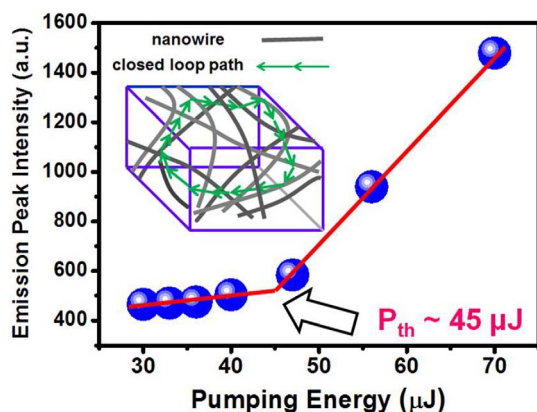


Figure 7 | Emission peak intensity of albumen-coated SnO₂ nanowires versus pumping energy. The inset illustrates the closed-loop path as a cavity for random laser.

state caused by impurities can produce the strong stimulated emission. In 1962, Rushba *et al.* first pointed out that the weakly bond exciton of impurities or defects can generate a giant oscillator strength, which is many orders larger than that of the free exciton²⁶. The wave function generated from the weakly bond exciton basically involves a whole region around defects, thus leads to the coherent oscillations of electrons^{14,26}. On the shallow-trapped state, there are many connected bond excitons²⁶, it is therefore believed that the stimulated emission can be well generated. This theoretical work provides an excellent foundation for the understanding of our observed behavior that the energy harvesting from FRET process can be efficiently turned into the UV emission arising from shallow defects in SnO₂ NWs.

In conclusion, we have demonstrated that a giant enhancement of 387 nm UV emission can be easily achieved from SnO₂ NWs by the assistance of UV-emitting (340 nm) chicken albumen protein at room temperature. The underlying mechanism is interpreted by the fluorescence resonance energy transfer (FRET), in which the energy can easily transfer from albumen protein (donor) to SnO₂ NWs (acceptor). Laser actions can be further derived from the albumen/SnO₂ NWs composite as well. Via a careful characterization, the laser action is believed to be the RL type lasing and is generated by the stimulated emission arising from the shallow-trapped state of SnO₂ NWs. The efficient transfer of energy harvesting from FRET process into UV emission is supported by theoretical work of extremely high oscillator strength of shallow defects in SnO₂ semiconductors. It is believed that our work shown here not only enables to open up the possibility of utilizing various biomolecule options for improving wide fields of light emitters, but also pave a new avenue towards future green bio-inspired optoelectronic devices.

Methods

Sample fabrication. The n-type SnO₂ nanowire arrays were grown on silicon (Si) substrates via vapor-liquid-solid (VLS) method. Prior to the growth, the single crystal Si substrates (0.5 cm × 0.5 cm) were ultrasonically cleaned for 10 min in acetone, ethanol and deionized (DI) water to remove any adsorbed contaminant. Next, Au thin film with a thickness of 10 nm was deposited on Si substrates by using a sputtering system (JFC-1600, JEOL). A high purity (99.99%) Sn metallic powder (1.5 g) was placed on a ceramic boat and the Au-coated Si substrate is nearby the powder. The boat was then loaded to the center of a horizontal tube furnace under the Argon gas with a flow rate of 200 sccm (sccm denotes cubic centimeter per minute at STP). After the above steps, the furnace temperature was elevated to 1000 °C rapidly at a rate of 100 °C min⁻¹. The sample was kept annealing for 10 min at 1000 °C. During the process, the vaporized Sn was reacted with oxygen and resulted in SnO₂ which blown onto the Au layer. As SnO₂ dissolved into Au, the nucleation occurred when the alloy of SnO₂-Au droplet reached supersaturation. After the furnace cooled down to room temperature, the as-grown white color SnO₂ NWs were obtained on Si substrate. Albumen liquid was obtained from chicken eggs purchased from a widely seen convenience store. After separating the egg yolk, the rest albumen liquid was directly used without any further purification or post baking. To fabricate our

albumen-coated SnO₂ NWs composite, the extracted albumen was spin-coated (5000 rpm) onto the as-grown SnO₂ NWs for 60 sec.

Morphology characterization and optical measurements. The morphologies of SnO₂ NWs and surface roughness of albumen were characterized by scanning electron microscope (SEM; JEOL JSM6500) and atomic force microscopy (AFM; Nanosurf Easyscan 2). The existence of SnO₂ NWs were confirmed by the Raman scattering measurement (Jobin Yvon T64000), X-ray diffraction (XRD; Panalytical X'pert PRO), and PL spectra were carried out by the excitation of 266 nm laser. The transmittance spectra of albumen with different spin-coating speed were detected with a spectrophotometer (Jobin-Yvon H10). To study the lasing behavior, the albumen-coated SnO₂ NWs were optically excited by a Q-switched 4th harmonic Nd:YAG laser (266 nm, 3–5 ns pulse, 10 Hz) and measured with a Jobin Yvon iHR550 imaging spectrometer system. The laser beam was focused to a diameter of about 300 μm. All of the luminescence experiments were performed at room temperature.

- Nizamoglu, S., Gather, M. C. & Yun, S. H. All-biomaterial laser using vitamin and biopolymers. *Adv. Mater.* **25**, 5988 (2013).
- Johnson, J. C. *et al.* Single gallium nitride nanowire lasers. *Nat. Mater.* **1**, 106–110 (2002).
- Vanmaekelbergh, D. & Vugt, L. K. ZnO nanowire lasers. *Nanoscale* **3**, 2783–2800 (2011).
- Yang, H. Y. *et al.* Ultraviolet coherent random lasing in randomly assembled SnO₂ nanowires. *Appl. Phys. Lett.* **94**, 241121 (2009).
- Heo, J., Jahangir, S., Xiao, B. & Bhattacharya, P. Room-temperature polariton lasing from GaN nanowire array clad by dielectric microcavity. *Nano. Lett.* **13**, 2376–2380 (2013).
- Saxena, D. *et al.* Optically pumped room-temperature GaAs nanowire lasers. *Nat. Photonics* **7**, 963–968 (2013).
- Li, J. *et al.* Wavelength tunable CdSe nanowire lasers based on the absorption-emission-absorption process. *Adv. Mater.* **25**, 833–837 (2013).
- Yeh, P. H., Li, Z. & Wang, Z. L. Schottky-gated probe-free ZnO nanowire biosensor. *Adv. Mater.* **21**, 4975–4978 (2009).
- Motayed, A. *et al.* Diameter dependent transport properties of gallium nitride nanowire field effect transistors. *Appl. Phys. Lett.* **90**, 043104 (2007).
- Wan, Q. *et al.* Fabrication and ethanol sensing characteristics of ZnO nanowire gas sensor. *Appl. Phys. Lett.* **84**, 3654 (2004).
- Krogstrup, P. *et al.* Single nanowire solar cells beyond the Shockley-queisser limit. *Nat. Photonics* **7**, 306–310 (2013).
- Li, Y. *et al.* Realizing a SnO₂-based ultraviolet light-emitting diode via breaking the dipole-forbidden rule. *Npg. Asia. Mater.* **4**, e30 (2012).
- Zhou, W. *et al.* Bound exciton and optical properties of SnO₂ one-dimensional nanostructures. *J. Phys. Chem. C* **113**, 1719–1726 (2009).
- Liu, R. B. *et al.* Stimulated emission from trapped excitons in SnO₂ nanowires. *Physica E* **39**, 223–229 (2007).
- Chen, I. T., Chang, P. H., Chang, Y. C. & Guo, T. F. Lighting up the ultraviolet fluorescence from chicken albumen through plasmon resonance energy transfer of gold nanoparticles. *Sci. Rep.* **3**, 1505 (2013).
- Chang, J. W. *et al.* Chicken albumen dielectrics in organic field-effect transistors. *Adv. Mater.* **23**, 4077–4081 (2011).
- Cerdán, L. *et al.* FRET-assisted laser emission in colloidal suspensions of dye-doped latex nanoparticles. *Nat. Photonics* **6**, 621–626 (2012).
- Berney, C. & Danuser, G. FRET or no FRET: A quantitative comparison. *Biophys. J.* **84**, 3992–4010 (2003).
- Sinha, A. K. *et al.* Tin oxide with a p-n heterojunction ensures both UV and visible light photocatalytic activity. *RSC. Adv.* **4**, 208–211 (2014).
- Wang, H. *et al.* Photochemical growth of nanoporous SnO₂ at the air-water interface and its high photocatalytic activity. *J. Mater. Chem.* **20**, 5641–5645 (2010).
- Huang, M. H. *et al.* Room-temperature ultraviolet nanowire nanolasers. *Science* **292**, 1897–1899 (2001).
- Chen, R., Lin, B., Sun, X. W. & Sun, H. D. Room temperature excitonic whispering gallery mode lasing from high-quality hexagonal ZnO microdisks. *Adv. Mater.* **23**, 2199–2204 (2011).
- Cao, H. *et al.* Random laser action in semiconductor powder. *Phys. Rev. Lett.* **82**, 2278–2281 (1999).
- Wang, C. S., Chang, T. Y., Lin, T. Y. & Chen, Y. F. Biologically inspired flexible quasi-single-mode random laser: An integration of *Pieris canidia* butterfly wing and semiconductors. *Sci. Rep.* **4**, 6736 (2014).
- Yang, H. Y., Yu, S. F., Li, G. P. & Wu, T. Random lasing action of randomly assembled ZnO nanowires with MgO coating. *Opt. Express* **18**, 13647–13654 (2010).
- Rashba, É. I. & Gurgenshvili, G. É. Edge absorption theory in semiconductors. *Sov. Phys. Solid State* **4**, 759–760 (1962).

Acknowledgments

This work was supported by the National Science Council and the Ministry of Education of the Republic of China.



Author contributions

C.S.W., T.Y.L. and Y.F.C. designed the experiment. C.S.L., T.M.S. and Y.C.C. reviewed the manuscript. C.S.W. performed the data measurements and wrote the manuscript. All authors contributed to the analysis and commend of the manuscript.

Additional information

Competing financial interests: The authors declare no competing financial interests.

How to cite this article: Wang, C.-S. *et al.* Biologically inspired band-edge laser action from

semiconductor with dipole-forbidden band-gap transition. *Sci. Rep.* 5, 8965; DOI:10.1038/srep08965 (2015).



This work is licensed under a Creative Commons Attribution 4.0 International License. The images or other third party material in this article are included in the article's Creative Commons license, unless indicated otherwise in the credit line; if the material is not included under the Creative Commons license, users will need to obtain permission from the license holder in order to reproduce the material. To view a copy of this license, visit <http://creativecommons.org/licenses/by/4.0/>